Spatial distribution of vortices and anisotropy of mutual friction in rotating He II

P. Mathieu, B. Plaçais, and Y. Simon
Groupe de Physique des Solides de l'Ecole Normale Supérieure
(Laboratoire associé au Centre National de la Recherche Scientifique),
24 rue Lhomond, F-75231 Paris Cedex 05, France
(Received 8 August 1983)

Accurate measurements of the attenuation of second sound in a rotating parallelepipedic cavity are reported. The cavity, which is used as a half-wave resonator, can be tilted about one of its symmetry axes so that the two large faces make an arbitrary angle θ with the angular velocity $\vec{\Omega}$. A continuum model is developed predicting that vortices, at equilibrium, must bend near the inclined plane walls, and terminate perpendicular to the boundary. The curvature of the vortices, otherwise parallel to $\vec{\Omega}$ and uniformly distributed, takes place over a characteristic depth $d_0=0.29\Omega^{-1/2}$ mm which is small compared with the dimensions of the cavity. The resulting changes in density and orientation of vortex lines, though localized near the walls, measurably affect the detailed dependence on both Ω and θ of the quality factors of resonant modes. Experimental results taken with two fundamental modes of the cavity support our model. As a by-product of these measurements we obtain information about the angular dependence of mutual friction. A small but clearly nonzero attenuation was observed for a second sound propagated in the direction of vortex lines. This axial attenuation can be described by introducing, besides the first mutual-friction parameter B, another dissipative coefficient B'' which is about 2.5% of B (at 1.9 K). In Hall and Vinen's equations of motion of He II this B'' should represent the axial component (along $\vec{\Omega}$) of the mutual-friction force. In this work we have deliberately ignored the intricate problem of metastable states, trying to get rid of them in experiments; thus reported results all refer to states of (or near) thermodynamic equilibrium.

I. INTRODUCTION

Except for surface effects such as the existence of a vortex-free region along the walls parallel to the angular velocity $\vec{\Omega}$, He II contained in a rotating vessel is expected to be threaded by an array of vortices parallel to $\vec{\Omega}$ and uniformly distributed with a density $n=2\Omega/\kappa$, where κ is the quantum of circulation.[1] As a result, the average superfluid velocity field imitates solid-body rotation: $\vec{\mathbf{V}}_s=\langle\vec{\mathbf{v}}_s\rangle=\vec{\Omega}\times\vec{\mathbf{r}}$.

To investigate the dynamical properties of vortices or to simply detect them, second sound has proved to be a very sensitive and versatile probe. Our present second-sound techique has already been described.[2,3] A parallelepipedic cavity serves both as a second-second resonator and as the rotating container. By accurately measuring the acoustical response of the rotating cavity for various modes, one obtains information about the spatial distribution. As shown in Ref. 2, a by-product of such measurements is a precise determination of mutual-friction coefficients. By tilting the cavity off the vertical axis of rotation, we observe new surface effects in the vortex distribution. Then, following for these surface effects in the data reduction, we were able to test the angular dependence of mutual friction to a higher degree of precision than has been achieved before.

As the size of the cavity (~ 1 cm), and accordingly the second-sound wavelength, are usually large compared with the vortex spacing ($n^{-1/2}\sim 0.1$ mm at $\Omega\sim 1$ sec^{-1}), rotating He II can be regarded as a continuous medium. The relevant macroscopic equations of motion were first proposed by Hall and Vinen,[4] and later derived phenomenologically by Bekarevich and Khalatnikov[1,5] (the HVBK equations). From this macroscopic point of view the bulk rotating He II, at thermodynamic equilibrium, appears as a homogeneous medium with constant density and orientation of vortex lines, to which we refer as *standard rotating helium.*

For a second-sound wave traveling perpendicular to vortices in standard rotating helium, the attenuation constant due to rotation, according to the HVBK theory, can be written

$$\alpha_v=B\Omega/2u_2\ , \tag{1}$$

where u_2 is the second-sound velocity, and B here is short for B_1, the real part of the first mutual-friction parameter.[3] If second sound is propagated at any angle θ to the vortex lines, B should be replaced in Eq. (1) by $B\sin^2\theta+B''\cos^2\theta$. The third mutual-friction parameter B'' was originally introduced in the HVBK equations to account for a possible small extra-attenuation of a second sound propagated parallel to vortices. Old experiments performed by Snyder and Putney[6] have confirmed the linear dependence of α_v as a function of $\sin^2\theta$; within the limits of experimental error, B'' was observed to be zero, a result since accepted as being consistent with microscopic models of mutual friction.[7]

As explained in Sec. II using minimum free-energy arguments, the vortex array, at equilibrium, must undergo a deformation near the walls that make arbitrary angles

with $\vec{\Omega}$. Associated vortex bending and low-density effects are predicted to extend over a characteristic distance d_0 from the walls, which is typically of the order of 0.1–1 mm.

In Sec. III it is shown that such a deformation of the vortex array in a rotating resonator, as well as the vortex-free region,[2] should result in small detectable changes in the quality factors of resonant modes, with respect to those expected from a cavity presumed to be entirely filled with standard rotating helium.

In Sec. IV we report accurate measurements of the variations of second-sound amplitudes in a rotating cavity as a function of Ω for various values of θ. Experimental results agree with theoretical predictions of Sec. II about the spatial distribution of vortices. Concerning the anisotropy of mutual friction, the most striking result is that B'', although small, is clearly nonzero. The paper ends with concluding remarks (Sec. V).

II. EQUILIBRIUM VORTEX DISTRIBUTION

Just as for an ordinary liquid, the equilibrium state of motion of He II in a uniformly rotating vessel minimizes the kinetic "free energy"

$$F=\int_{\text{cavity}}(E-\vec{M}\cdot\vec{\Omega})d^3r\ , \tag{2}$$

where E and $\vec{M}$ are, respectively, the kinetic energy and angular momentum density. In this section we shall show that the general equilibrium conditions for the vortex array readily follow from this minimum free-energy principle by using the HVBK continuum approximation. In Ref. 2, while carrying out a similar procedure, we only examined two-dimensional vortex motion. In this work the cavity walls are not restricted to being either parallel or perpendicular to the axis of rotation, and hence our problem is really a three-dimensional one.

Any distribution of vortices in the cavity will be described locally by two parameters n and $\vec{\nu}$ which may be functions of position: n is the vortex density and $\vec{\nu}$ is the unit vector along the vortex lines. n is usually defined as the number of lines crossing the unit area normal to vortices; it is connected to the radial dimension of the vortex cell b by the relation

$$n\pi b^2=1\ . \tag{3}$$

Equivalently, n can be seen as the total length of line per unit volume. The latter definition is most suitable to a three-dimensional description. The mean curl of the superfluid velocity, denoted as $\vec{\omega}$,[1] is simply related to n and $\vec{\nu}$,

$$\vec{\omega}=\text{curl}\vec{V}_s=n\kappa\vec{\nu}\ . \tag{4}$$

In standard rotating He II, $\vec{\omega}=2\vec{\Omega}$ with $n=n_0=2\Omega/\kappa$ and $\vec{\nu}=\vec{\nu}_0=\vec{\Omega}/\Omega$.

Regarding the normal and superfluid densities ρ_n and ρ_s as constants, the kinetic energy density in Eq. (2) can be expressed as

$$E=\tfrac{1}{2}\rho_s V_s^2+\tfrac{1}{2}\rho_n V_n^2+n\,\Delta E\ , \tag{5}$$

where ΔE is a vortex energy per unit length of line,[1,2]

$$\Delta E=\frac{\rho_s\kappa^2}{4\pi}\left[\ln\frac{b}{a}-\frac{1}{4}\right]\ . \tag{6}$$

Here a is the effective core radius ($a\simeq 10$ Å).[2] In squaring the mean superfluid velocity $\vec{V}_s$ one underestimates the contribution to the kinetic energy of large local velocities $\vec{v}_s$ around the vortex cores. Hence, ΔE appears as a positive correction term, allowing for the finite and discrete character of vorticity. Upon differentiating Eq. (5) we obtain

$$dE=\rho_s\vec{V}_s\cdot d\vec{V}_s+\rho_n\vec{V}_n\cdot d\vec{V}_n+\rho_s\Lambda\vec{\nu}\cdot d\vec{\omega}\ , \tag{7}$$

where

$$\Lambda=\frac{\kappa}{4\pi}\ln(b^*/a),\quad b^*=be^{-3/4}\ . \tag{8}$$

It will also be useful to introduce the characteristic length

$$d_0=(\Lambda/\Omega)^{1/2}\ , \tag{9}$$

where Λ is taken with the standard value of b [$b=(n_0\pi)^{-1/2}$]. In the two-dimensional problem investigated in Ref. 2, the vortex distribution appeared as a uniform standard continuum ($n=n_0$), leaving along the walls parallel to $\vec{\Omega}$ a vortex-free layer ($n=0$) of constant width. In thermodynamic equilibrium, the calculated thickness of this vortex-free layer was precisely found to be d_0 [see Eq. (23) of Ref. 2], in agreement with experiment.

We could have left out the small and commonly omitted terms of order of or less than unity in Eqs. (6) and (8). In the BK expression for the differential of the internal energy, the last term of Eq. (7) is written as $\lambda\,d\omega$, where λ is, to within logarithmic accuracy, equal to $(\rho_s\kappa/4\pi)\ln(b/a)$.[15] In the same range of accuracy we may ignore a small quantum correction in the angular momentum density $\vec{M}$,[2] of order $\rho_s\kappa/4\pi$, so that $\vec{M}$ reduces to macroscopic terms,

$$\vec{M}=\vec{r}\times(\rho_n\vec{V}_n+\rho_s\vec{V}_s)\ . \tag{10}$$

Equilibrium requires that $\delta F=0$ for arbitrary variations $\delta\vec{V}_n$ and $\delta\vec{V}_s$, in particular for a $\delta\vec{V}_s$ resulting from a virtual change in the spatial distribution of vortices ($\delta\vec{\omega}=\text{curl}\,\delta\vec{V}_s$). Note that $\delta\vec{V}_s$ is not necessarily zero at the boundaries. Substituting the expressions given above for E and $\vec{M}$ in Eq. (2), an elementary calculation yields

$$\begin{aligned}\delta F=&\rho_n\int\delta\vec{V}_n\cdot(\vec{V}_n-\vec{\Omega}\times\vec{r})d^3r\\&+\rho_s\int\delta\vec{V}_s\cdot[\vec{V}_s+\text{curl}\,(\Lambda\vec{\nu})-\vec{\Omega}\times\vec{r}\,]d^3r\\&+\rho_s\int_{\text{walls}}\delta\vec{V}_s\cdot(\Lambda\vec{\nu}\times\vec{N})d^2r\ ,\end{aligned}$$

where $\vec{N}$ is the unit vector normal to the boundary. Thus we get the local equilibrium conditions,

$$\vec{\nu}\times\vec{N}=0\ , \tag{11}$$

$$\vec{V}_n=\vec{V}_s+\text{curl}(\Lambda\vec{\nu})=\vec{\Omega}\times\vec{r}\ . \tag{12}$$

Taking the curl of Eq. (12), we obtain an equilibrium condition for n and $\vec{\nu}$,

$$n\kappa\vec{v}+\mathrm{curl}\,\mathrm{curl}(\Lambda\vec{v})=2\vec{\Omega}=n_0\kappa\vec{v}_n\ . \tag{13}$$

Equation (11) implies that vortices must end normal to the container walls, and since they have to be parallel to $\vec{\Omega}$ in the bulk, the lines will inevitably be curved (Fig. 1). Note that Eqs. (12) and (13) no not exclude vortex bending ($\mathrm{curl}\vec{v}\neq 0$). Equation (12) is consistent with the fact that the quantity $\rho_s[\vec{V}_s-\vec{V}_n+\mathrm{curl}(\Lambda\vec{v})]$ appears as an affinity in the BK expression for the dissipative function.[5]

Equations (11) and (12) can be easily interpreted on a microscopic scale by considering the behavior of isolated vortex lines. The quantity $\vec{V}_s+\mathrm{curl}(\Lambda\vec{v})$ is a macroscopic expression for the local superfluid velocity $\vec{v}_s^*$ induced at the core of a given vortex by all other vortices and by the vortex itself if it is curved; $\vec{v}_s^*$ coincides with the average velocity $\vec{V}_s$ only for a regular array of rectilinear vortices that induce no velocity at their center. Equation (12) thus states that $\vec{v}_s^*$ equals the local normal velocity $\vec{v}_n=\vec{V}_n$, which is the physical condition for having no mutual friction. On the other hand, unless normal to the boundary, a vortex continued by its own image behaves as a vortex with infinite curvature. Close to the walls, very large velocities $\vec{v}_s^*$ incompatible with equilibrium are induced by the image vortex.

Though somewhat more complicated, Eq. (13) is similar to the London equation for the magnetic field $\vec{h}$ in a superconductor,[8]

$$\vec{h}/\lambda^2+\mathrm{curl}\,\mathrm{curl}\,\vec{h}=0\ .$$

This equation involves the exponential decrease of $\vec{h}$ toward the interior of the superconductor, $\vec{h}$ falling off to the bulk value zero over a penetration depth λ. Similarly, Eq. (13) implies that $\vec{v}$ rapidly changes direction from the normal $\vec{N}$ to the bulk value $\vec{v}_0$ over a characteristic depth of the order of $(\Lambda/n\kappa)^{1/2}$ or d_0, namely a few tenths of millimeters. On the scale of our containers (~ 1 cm), the curvature of vortices therefore appears as a surface effect. Everywhere beyond a small layer of thickness d_0 along the walls, the vortex array recovers its standard equilibrium conditions ($n=n_0$, $\vec{v}=\vec{v}_0$).

Now we wish to emphasize that a decrease in vortex density is expected to be associated with the curvature of vortices in the perturbed layer d_0. Consider, for example, the $z=0$ plane wall of the parallelepipedic cavity shown in Fig. 1. The vector $\vec{\Omega}$ lies in the xz plane and makes the angle θ with the wall. The structure of the vortex array in the vicinity of the $z=0$ plane will be described in the continuum approximation by a one-dimensional solution of Eq. (13), where n and $\vec{v}$ are functions only of z. For the vortex lines lying in the xz planes, let $\phi(z)$ be the angle between the line and the x axis ($v_x=\cos\phi$, $v_z=\sin\phi$); $\phi(0)=\pi/2$ and $\phi(z\gtrsim d_0)\simeq\theta$. Upon taking the z component of Eq. (13) we find

$$n\sin\phi=n_0\sin\theta\ . \tag{14}$$

It follows that the vortex density near the wall, $n(0)=n_0\sin\theta$, is lower than the bulk density n_0. The decrease in vortex density appears as a simple geometrical effect, which is noticed at once in sketching the vortex array as illustrated in Fig. 1 for $\theta=20°$. As θ approaches zero, n vanishes as far as $\phi\neq\theta$, i.e., as far as $z\lesssim d_0$. Thus we retrieve as a limiting case the existence of a vortex-free layer d_0 along a plane wall parallel to $\vec{\Omega}$. This will become quantitatively clear in the calculations of Sec. III.

We are justified in neglecting the slight logarithmic dependence of Λ on the vortex density. Even for $\theta=10°$, which, except for zero, was the smallest tested angle, the relative variation of Λ does not exceed 10%. Therefore, regarding Λ as a constant in Eq. (13) ($\Lambda=\Omega d_0^2$) and substituting n from Eq. (14) in the x component of Eq. (13), we obtain

$$\frac{\sin\theta}{\tan\phi}-\frac{d_0^2}{2}\frac{d^2(\cos\phi)}{dz^2}=\cos\theta\ . \tag{15}$$

Upon multiplying Eq. (15) by $d(\cos\phi)/dz$ and integrating, we find

$$\frac{d\phi}{dz}=-\frac{\sin[(\phi-\theta)/2]}{\sin\phi}\frac{2\sqrt{2}}{d_0}\ . \tag{16}$$

This differential equation for ϕ will be used in the second-sound acoustics of Sec. III when calculating the quality factors of two fundamental modes as functions of Ω and θ. From Eq. (16) the profile of the lines can be derived easily in a parametric form, $x(\phi)$ and $z(\phi)$. These parametric equations, which otherwise are not worth writing, confirm the rapid change in orientation of the vortex lines over the distance d_0. For instance, with $\theta=20°$, which is the case of Fig. 1, $\phi=30°$ at the distance $z=d_0$ from the wall, and $\phi=21°$ at $z=1.7d_0$.

As d_0 is not much larger than the interline distance, one might question the relevance of the HVBK model. However, the quantitative agreement between second-sound data and predictions of the continuum model concerning

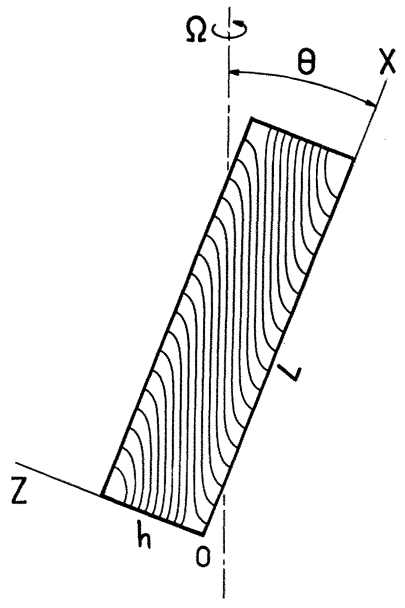

FIG. 1. Cross section of the parallelepipedic rotating cavity and schematic of the model vortex distribution showing the decrease in vortex density along the inclined walls. The cavity is used as a half-wave resonator by exciting either the x or the y fundamental mode.

the vortex-free layers,[2] has given us some confidence in the present macroscopic approach. Also, we refer the reader to the paper of Campbell and Ziff,[9] where the authors calculate equilibrium vortex patterns in a rotating cylinder for relatively small numbers of vortices; by merely inspecting the stable pattern of 217 vortices shown in Fig. 5 of Ref. 9, one realizes the physical reality of a vortex-free region surrounding a uniformly spaced array of vortices.

III. SECOND-SOUND ACOUSTICS AND EXPERIMENTAL PRINCIPLE

The rotating cavity of Fig. 1 is a rectangular parallelepipedic box whose internal dimensions will be denoted L, l, and h. For the discussion we have taken a coordinate system attached to the box; the x, y, and z axes are chosen to be along the L, l, and h sides, respectively, as shown in Fig. 1. The cavity can be tilted about one of its symmetry axes so that the xz planes remain vertical. Standing waves of second sound may be set up along either x or y axis.

First, suppose the cavity is to be driven on its fundamental x mode. The amplitude of the temperature field can then be written as

$$T_1 = A\left[1+iQ\frac{\omega-\omega_x}{\omega_x}\right]^{-1}\cos\left[\frac{\pi x}{L}\right], \tag{17}$$

where ω_x is the resonance frequency and Q is the quality factor of the mode. The wave velocity field, $\vec{V}_{n1}-\vec{V}_{s1} \propto \vec{\nabla} T_1$, lies parallel to the x direction and has nodes on the faces $x=0$ and L,

$$\vec{V}_{n1}-\vec{V}_{s1}=(\rho/\rho_s)\vec{V}_{n1}\propto \sin(\pi x/L)\ . \tag{18}$$

From the response curve $T_1(\omega)$ measured at $x=0$ or L,[3] the maximum resonant amplitude A and the quality factor Q can be determined. A is proportional to Q so that $A/A_0=Q/Q_0$, where A_0 and Q_0 refer to the stationary resonator.

In the absence of spurious coupling between the cavity and the external bath, Q^{-1} is in turn proportional to the power lost in the cavity. At the working temperature and sound frequency ($T\simeq 1.9$ K; $\omega/2\pi\sim 10^2-10^3$ Hz) the normal-fluid viscosity turns out to be the prevailing dissipative mechanism for both surface losses and mutual friction. In the resonator at rest, volume losses are negligibly small and power loss takes place at cavity walls within a thin viscous boundary layer; its thickness δ, i.e., the viscous penetration depth of the normal fluid, is of the order of a few micrometers. In a rotating resonator, small oscillations of vortices subject to the velocity field of second sound entail a local perturbation of the normal flow around the vortex over a distance which again is of the order of δ; the dissipative process of mutual friction is none other than the viscosity of the dragged normal fluid.[10] Mutual friction interferes with surface viscosity within a negligible fraction, $\delta^2/b^2\sim 10^{-13}$, of the boundary layers. Therefore, within the accuracy of our measurements, Q^{-1} may be expressed as the sum of two independent additive terms,

$$1/Q=1/Q_0+1/Q_v\ , \tag{19}$$

where Q_0^{-1} represents surface losses, such as measured at $\Omega=0$, and Q_v^{-1} is the vortex contribution. Q_v is the quality factor that would result if the only source of damping was mutual friction. Its experimental value will be obtained from resonance data by the relation

$$\frac{1}{Q_v}=\frac{1}{Q_0}\left[\frac{A_0}{A}-1\right]. \tag{20}$$

The problem then is to calculate, for comparison with experiment, the theoretical value of Q_v^{-1} by taking into account the details of the vortex distribution near the boundaries. This calculation has been made in Ref. 2 in the two-dimensional case $\theta=\pi/2$, and has to be generalized for any value of the tilting angle θ.

According to the model of Sec. II, the vortex distribution is expected to deviate from the standard conditions ($n=n_0$, $\vec{v}=\vec{v}_0$) within a sheath of thickness d_0 along the cavity walls. The two vortex-free layers of constant thickness d_0 should form along the vertical faces $y=0$ and l, and vortex bending should occur near the other four faces as shown in Fig. 1. Every element of vortex line contributes to energy dissipation according to its position and orientation in the standing wave. For lines making an angle α with the direction of sound, the power dissipation per unit length of line is

$$\frac{1}{2}\frac{\rho_n\rho}{\rho}\kappa B(\alpha)V_{n1}^2\ , \tag{21}$$

where we have introduced an angular-dependent mutual-friction parameter $B(\alpha)$ with the short notation

$$B(\alpha)=B\sin^2\alpha+B''\cos^2\alpha=C\sin^2\alpha+B''\ , \tag{22}$$

where $C=B-B''$. In the continuum approximation, the vortex term Q_v^{-1} calculated for the x mode can be written in the form

$$Q_v^{-1}=k\int nB(\alpha)\sin^2(\pi x/L)d^3r\ . \tag{23}$$

Let us note that $\delta\ll d_0$ so that we may ignore the falling off of $\vec{V}_{n1}$ at the boundaries.

By assuming the cavity to be entirely filled with standard rotating helium ($n=n_0$, $\alpha=\theta$), we must derive the known classical result such as derived from HVBK equations,[6]

$$1/Q_{vs}=B(\theta)\Omega/2\omega=\alpha_y L/\pi\ . \tag{24}$$

Hence, we have $k=\kappa/2\omega V$, where $V=Llh$ is the volume of the cavity. Effects of the vortex-free or perturbed layers d_0 should consist in small deviations of Q_v^{-1} from the standard value (24) of the order of d_0/h, d_0/l, or d_0/L. In reducing the experimental data it will be convenient to define an apparent mutual-friction parameter denoted as B^* by setting, in any case,

$$1/Q_v=\frac{B^*\Omega}{2\omega}\ . \tag{25}$$

As $n=0$ outside the interval $d_0<y<l-d_0$ and is otherwise independent of y, the integration over y in Eq. (23) yields a factor $l-2d_0$. On the other hand, vortices close to the walls $x=0$ and L, whether curved or not, are undetected by the x mode which has nodes there. Therefore,

we may disregard the x dependence of n and α in the integral (23), and refer to the one-dimensional solution $n(z)$ and $\alpha=\phi(z)$ investigated in Sec. II. It follows that

$$B^*=\gamma_x\frac{1}{n_0h}\int_0^h n(z)B(\phi)dz\ , \tag{26}$$

where $\gamma_x=1-2d_0/l$ is the filling factor introduced in Ref. 2. The integral in Eq. (26) is readily evaluated by writing it as the sum of a standard term and two equal layer corrections,

$$\frac{B^*}{\gamma_x}=B(\theta)+\frac{2}{n_0h}\int_{\pi/2}^{\theta}[n(\phi)B(\phi)-n_0B(\theta)]\frac{dz}{d\phi}d\phi\ .$$

After substituting n and $dz/d\phi$ as a function of ϕ from Eqs. (14) and (16), a lengthy but elementary calculation yields

$$B^*=\gamma_x\{B(\theta)+(2d_0/h)[Cf(\theta)+B''g(\theta)]\}\ , \tag{27}$$

where $f(\theta)$ and $g(\theta)$ are two trigonometric expressions of order unity,

$$f(\theta)=\frac{\sin\theta}{3\sqrt{2}}\left[\cos2\theta-2\cos\left[\frac{\pi}{4}-\frac{\theta}{2}\right]+3\right]\ , \tag{28}$$

$$g(\theta)=\sqrt{2}\left[\sin\theta-\sin\left[\frac{\pi}{4}+\frac{\theta}{2}\right]\right]\ . \tag{29}$$

By systematically neglecting the terms of second order in the small quantities d_0/l, d_0/h, and B''/B in Eq. (27), we obtain the following simplified expression for B^* that we shall use in fitting the experimental data:

$$B^*=B(\theta)-(2d_0/l)B\sin^2\theta+(2d_0/h)Bf(\theta)\ . \tag{30}$$

The first correcting term in Eq. (30) is negative and represents the effect (of order $2d_0/l$) of the missing vortices along the walls $y=0$ and l. It should be emphasized that the last term turns out to be positive [$f>0$ except that $f(0)=f(\pi/2)=0$]. The decrease in vortex density in the two perturbed layers $z=0$ and h, should tend to decrease the attenuation of sound just as a vortex-free layer. However, bent vortices, if shorter than standard vortices, also tend to become perpendicular to the direction of second-sound propagation. In other words, while the total length of lines is decreased, the power lost per unit length of line is increased. The calculation shows that the latter effect must prevail.

Now the same procedure can be employed to calculate the theoretical value of Q_v^{-1} for the y fundamental mode: $T_1\propto\cos\pi y/l$, $\vec{V}_{n1}\propto\sin\pi y/l$. Since the vortices in this case are normal everywhere to the direction of propagation of sound, there will be no anisotropy effect ($\alpha=\pi/2$), and we can write

$$Q_v^{-1}=\frac{k}{2\omega V}\int Bn(\vec{r})\sin^2(\pi y/l)d^3r\ . \tag{31}$$

The y mode does not "see" the vortex-free layers near its nodes at $y=0$ and l. Thus, ignoring the y dependence of n, the integration over y in Eq. (31) yields the factor $l/2$. Compared to its standard value, the quality factor of the y mode will be affected only by the reduction of vortex density in the four perturbed layers. This amounts to reducing the apparent value of the mutual-friction parameter,

$$B^*=B\left[1+\frac{1}{n_0Lh}\int(n-n_0)dx\,dz\right]\ , \tag{32}$$

where the integral correction is zero outside the four layers. Neglecting corner effects, which involve terms of the order of $d_0/Lh\lesssim10^{-3}$, we can calculate the integral as the sum of four independent terms by using the one-dimensional solution of Sec. II. This solution applies to the layers $x=0$ and L by simply exchanging x and z, h and L, and θ and $\pi/2-\theta$. We thus find for the y mode

$$B^*=B[1+(2d_0/h)g(\theta)+(2d_0/L)g(\pi/2-\theta)]\ . \tag{33}$$

As is easily seen from Eq. (29), $g(\theta)$ is a strictly increasing function of θ throughout the interval $0<\theta<\pi/2$, from $g(0)=-1$ to $g(\pi/2)=0$. Hence the correcting terms in Eq. (33) are negative, as they should be. As θ tends to zero, Eq. (33) reduces to $B^*=B(1-2d_0/h)$, which is the expression to be expected in the presence of two vortex-free layers of thickness d_0 along the planes $z=0$ and h. This confirms quantitively our assertion in Sec. II that the vortex-free layer can be regarded by continuity as a limiting case of the one-dimensional perturbed layer.

For further reference and comparison with experiment we collect the results derived for both modes below. The deviation of the vortex distribution from standard conditions will result in a deviation of Q_v^{-1} from its standard value (24), which has been equivalently expressed in terms of a deviation ΔB^* of the apparent mutual-friction parameter, such as that given directly by experiment from the standard value; that is, $B(\theta)$ for the x mode and B for the y mode. Equations (30) and (33) can be rewritten as

$$\Delta B^*/B=-(2d_0/l)\sin^2\theta+(2d_0/h)f(\theta)\ , \tag{34}$$

$$\Delta B^*/B=(2d_0/h)g(\theta)+(2d_0/L)g(\pi/2-\theta)\ , \tag{35}$$

for the x and y modes, respectively. All vortex-distribution effects, whether due to missing or curved vortices, are proportional to d_0, and according to Eq. (9), vanish at large angular velocities. The Ω dependence of B^* is that of d_0. The logarithmic factor $\Lambda^{1/2}$ in d_0 only varies by a few percent in the investigated range of angular velocities ($0.3\lesssim\Omega\lesssim10\ \mathrm{sec}^{-1}$), so that it may be approximately regarded as constant. Expressing d_0 in mm,

$$d_0=(0.29\pm0.01)\Omega^{-1/2}\ . \tag{36}$$

Earlier measurements of B^*,[2] in cavities having walls either parallel or normal to $\vec{\Omega}$, have clearly demonstrated the existence of vortex-free layers of uniform width d along the vertical walls. Provided that thermodynamic equilibrium was achieved, $d=d_0$ and formula (36) proved correct. As shown in Ref. 2, however, d can take any value between two external values d_1 and d_2, depending on the past history of the rotating sample. Accordingly, the total number of vortices at constant density n_0 can fluctuate around its equilibrium value. At 1.9 K for a set of rectangular resonators we found $d_1\simeq1.6d_0$ and $d_2\simeq0.6d_0$. In the tilted resonator of Fig. 1, we must be aware that metastability still may alter the two vortex-free

layers along $y=0$ and l, the first correcting term in Eq. (34) varying as $2d/l$.

The effects of curved vortices near the planes $z=0$ and h are contained in terms proportional to $2d_0/h$ in Eqs. (34) and (35). In order to enhance these effects, the dimension h should be taken as small as possible. Typically with $h=3$ mm (and $d_0=0.3$ mm at $\Omega\simeq 1$ sec^{-1}), $\Delta B^*/B$ should be of the order of $d_0/h=10\%$.

IV. EXPERIMENTAL RESULTS

In addition to the fact that the investigated cavity can be tilted to the rotation axis through $\pm 180°$, the experimental technique, from the manner of making resonators to that of recording resonance curves, is quite similar to that described in previous papers,[2,3] The angle θ can be set to within $\pm 0.5°$ by means of a system of gear wheels which can be operated without stopping the rotation.

Two parallelepipedic cavities were specially designed for the present work; their internal dimensions are $L=47$ mm, $l=20$ mm, and $h=3$ or 6 mm. The cavity walls were machined from slabs of epoxy resin, and tightly bonded with an epoxy-resin adhesive. As explained in Ref. 3, leaks coupling the helium inside the cavity with the external bath, unless placed at nodes of temperature, may strongly affect the second-sound response and lead to unreliable results. The only links between the cavity and the helium bath are small holes drilled through the walls at $x=L/2$, and $y=l/2$, which is a temperature node for both the x and y fundamental modes. In the present experiment the observed constancy of Q_0 (or A_0) to better than 10^{-3}, while θ is varied through $\pm 180°$, was a sensitive test of the absence of external coupling.

All measurements were carried out at the same temperature, $T=1.875$ K, taking advantage of the optimum performance at about 1.9 K of our temperature control system.[3] At this temperature the resonance frequencies and the quality factors at rest of each of the two cavities were the following: for the x mode, $\omega_x/2=206$ Hz, $Q_0=1260$ ($h=3$ mm), and $Q_0=2335$ ($h=6$ mm); for the y mode, $\omega_y/2=485$ Hz, $Q_0=1920$ ($h=3$ mm), and $Q_0=3910$ ($h=6$ mm).

The resonant amplitudes of the x and y modes were measured accurately for various values of θ and Ω, while carefully controlling all other parameters involved: the ac input power, the driving frequency, and the bath temperature. At given Ω and θ, the apparent mutual-friction parameter B^* was calculated from the amplitude ratio A_0/A (and Q_0, ω, and Ω) through Eqs. (20) and (25).

We shall first discuss the results obtained with the x mode. θ being fixed, B^* was determined for several angular velocities ranging from $\Omega=0.3$ to 10 sec^{-1}. In all cases we observed the predicted linear dependence of B^* on $\Omega^{-1/2}$ in agreement with Eqs. (34) and (36). Figure 2 shows, for instance, the B^*-vs-$\Omega^{-1/2}$ data taken with the 3-mm cavity in the position sketched in Fig. 1 ($\theta\simeq 20°$). Upon extrapolating to $\Omega=\infty$ we eliminate any vortex-distribution effects, with the zero intercept of the fitting line yielding a precise value of the angular-dependent mutual-friction parameter $B(\theta)$. By collecting the values of $B(\theta)$ obtained in this way and plotting them as a function of $\sin^2\theta$, it is seen that the data are remarkably accounted for by the linear law

$$B(\theta)=0.021+0.834\sin^2\theta\ , \tag{37}$$

in accordance with Eq. (22). In particular,

$$B(0)=B''=0.021\pm 0.001,\quad B(\pi/2)=B=0.855\pm 0.005\ ,$$

at 1.875 K and 200 Hz. Figure 3 shows the low-angle part of the $B(\theta)$ line so as to emphasize the undeniably nonzero value of B''. The value $B''=0.021$ was found to be independent of the cavity size, as it should be. Note that small misalignments of the cavity could not affect the precise determination of B'', especially as $\sin^2\theta$ or $B(\theta)$ has a minimum at $\theta=0°$. The smallness of B'' (2.5% of B) may explain why it had previously escaped detection.[6,7] In the HVBK theory, B'' represents the magnitude of the axial component (along $\vec{\Omega}$) of the mutual-friction force. The existence of $B''\neq 0$, however small it may be, should give rise to serious theoretical problems, and requires further experimental investigation (see concluding remarks of Sec. V).

The slopes of the fitting lines B^* vs $\Omega^{-1/2}$ at various angles give information on the detailed vortex distribution along the boundaries. In this respect, the most significant feature of our results is the observation of positive slopes. Whereas the effect of missing vortices always tends to decrease the attenuation of sound ($\Delta B^*<0$), positive deviations ΔB^*, according to predictions of Sec. III, characterize the predominant effect of curvature of the vortices near the planes $z=0$ and h. Upon subtracting from the experimental value of $\Delta B^*/B$ the calculating negative

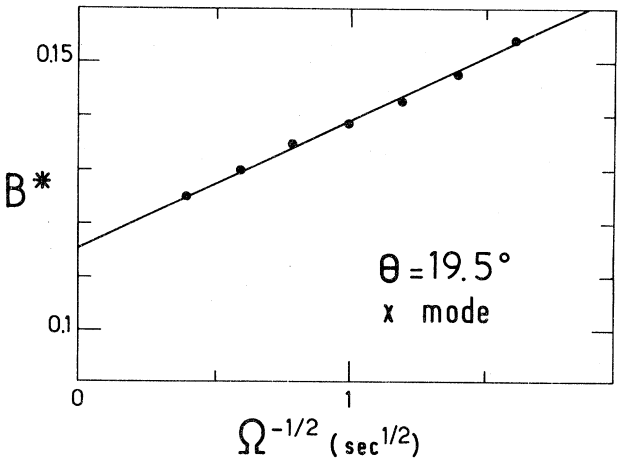

FIG. 2. Apparent mutual-friction parameter B^*, as defined by Eq. (25), as a function of the angular velocity. The linear dependence of B^* on $\Omega^{-1/2}$ is predicted by the theory of Secs. II and III. This figure shows B^*-vs-$\Omega^{-1/2}$ data taken at 1.875 K with the x mode of the cavity measuring $47\times 20\times 3$ mm^3. Upon extrapolating the fitting line to $\Omega=\infty$, we obtain the value of the angular-dependent parameter $B(\theta)=B\sin^2\theta+B''\cos^2\theta$ for $\theta=19.5°$, i.e., $B(\theta)=0.115\pm 0.002$. B^* is proportional to the average dissipated power due to vortices, and would be equal to $B(\theta)$ for a standard array of vortices uniformly distributed throughout the cavity. The increase of attenuation observed with the x mode [$B^*>B(\theta)$] is explained by the curvature of vortices near the planes $z=0$ and h (Fig. 1), which makes them become perpendicular to the direction of sound.

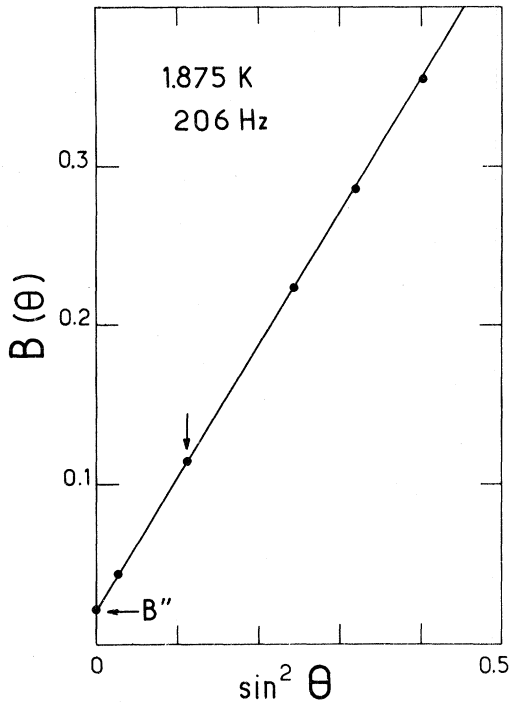

FIG. 3. Anisotropy of mutual friction at 1.875 K. The angular-dependent mutual-friction parameter $B(\theta)$ is plotted as function of $\sin^2\theta$ for low values of the tilting angle θ showing the nonzero intercept of the fitting line. The data are taken with the x mode of the 3-mm cavity ($\omega/2\pi=206$ Hz). The arrow marks the point deduced from data in Fig. 2 ($\theta\simeq 20°$). The straight-line dependence is predicted by the HVBK theory: $B(\theta)=B\sin^2\theta+B''\cos^2\theta$ by taking $B=0.855$ and $B''=0.021$.

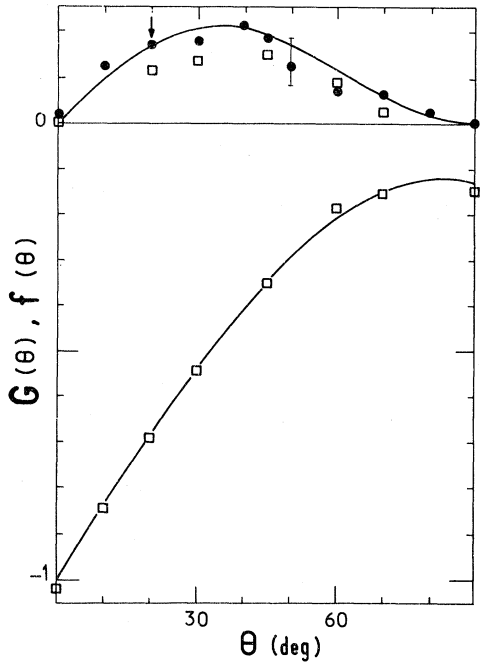

FIG. 4. $f(\theta)$ for the x mode (upper panel) and $G(\theta)$ for the y mode (lower panel) are dimensionless coefficients measuring the variations of the attenuation of second sound due to the bending of vortices near the cavity walls. According to Eqs. (34) and (35) the variation of the apparent mutual-friction parameter B^* associated with curvature effects is obtained on multiplying f or G by $2d_0/h$, then by B. The circles are experimental data taken with the 3-mm cavity ($h=3$ mm); the arrow marks the point obtained from the positive slope of the fitting line of Fig. 2 ($\theta\simeq 20°$). The open squares correspond to the 6-mm cavity. The upper and lower solid lines are theoretical curves deduced from trigonometric expressions (28) and (29) for $f(\theta)$ and $g(\theta)$, and definition of $G(\theta)$ by Eq. (39).

correction due to vortex-free layers, i.e., $-2d_0/l\sin^2\theta$, then dividing by $2d_0/h$, we obtain an experimental value of the angular-dependent coefficient $f(\theta)$. The $f(\theta)$-vs-θ data reported in Fig. 4 for both cavities are in fair agreement with the theoretical expression (28) for $f(\theta)$ (upper line in the figure).

We stress that all data reported in this paper refer to states of (or near) thermodynamic equilibrium. Metastability may considerably alter the small effects of anisotropy and vortex distribution which we are dealing with. We do not wish to discuss the intricate behavior of metastable states, here if only to avoid obscuring the simplicity and the coherence of the results related to equilibrium. However, we must consider metastability as a possible source of experimental error. In particular, as stated in Sec. II, the easy occurrence of metastable states associated with fluctuating numbers of vortices may scatter the measured values of B^* specially in the low-velocity range, making the slope of the fitting line B^* vs $\Omega^{-1/2}$ uncertain. In each case the rotation was rapidly set to the desired velocity Ω, either starting from zero or decelerating from some higher value. From previous measurements[2] we know that such a procedure tends to bring the rotating system closer to the state of thermodynamic equilibrium. Nevertheless, to ensure that we actually observe the equilibrium state, we ought to test its stability against strong disturbances such as jarring the cryostat or momentarily feeding a large dc heat flux in the cavity. It would also be useful to record, around each value of Ω, a hysteresis loop enclosing the equilibrium state.[2] While taking the data of Fig. 2 we took great care to achieving equilibrium. However, to save time we had to give up systematic testing. This explains the comparatively large scatter of the experimental values of $f(\theta)$. The error bar shown in Fig. 4, for example, has been calculated on the assumption that the thickness d of the vortex-free layers could take its extermal values d_1 and d_2 (see Sec. III). Moreover, since the main term in B^*, that is, $B\sin^2\theta$, is strongly angular independent, small accidental variations of θ may also give rise to additional experimental scatter. The relative lack of precision in the experimental $f(\theta)$ justifies the approximations made in deriving Eq. (30) from Eq. (27).

We now consider the results obtained with the y mode. The situation turns out to be simpler for two reasons: (i) By restricting ourselves to sound propagating normal to vortices we exclude anisotropy effects, and (ii) the vortex-free layers at $y=0$ and l being at velocity modes will be undetected. Therefore, the distribution effects appear only in the decrease of the vortex density along the four other walls. As expected, the fitting lines B^* vs $\Omega^{-1/2}$ for various angles θ all have negative slopes and a common intercept at $\Omega=\infty$,

$$B^*=0.890+m(\theta)\Omega^{-1/2}\,. \tag{38}$$

Hence we obtain $B=0.890$ at 1.875 K and 500 Hz. The difference between this value of B and that found with the x mode is well accounted for by the slow logarithmic dependence of B on sound frequency. According to both theory[10] and experiment,[3] at 1.9 K,

$$B^{-1}=\text{const}-5.3\times10^{-2}\ln\omega\ .$$

Let $G(\theta)$ be the relative variation $\Delta B^*/B$ expressed in units $2d_0/h$. Equation (34) predicts the θ dependence

$$G(\theta)=g(\theta)+\frac{h}{L}g(\pi/2-\theta)\ , \tag{39}$$

where $g(\theta)$ is given by Eq. (29). For both cavities experimental values of $G(\theta)$, in direct ratio to the slopes $m(\theta)$, are found to be in very good agreement with the theoretical expression (39). Note that $G(\theta)$ is slightly dependent on the aspect ratio h/L. Thus, for clarity, Fig. 4 shows only experimental $G(\theta)$ taken with the 6-mm cavity; the lower line in the figure has been calculated from Eq. (39) taking $h=6$ mm and $L=47$ mm.

V. CONCLUSIONS

The data obtained with both modes provide, as a whole, convincing evidence that vortices near the walls do behave as schematically shown in Fig. 1. The agreement of our results with the detailed predictions of Sec. II and III support the correctness of the basic equilibrium conditions (11) and (12) underlying them, and of the original Λ term in the BK expression for the free energy. It should be pointed out that the model of Sec. II not only accounts for the linear dependence of B^* on $\Omega^{-1/2}$ and the form of the θ dependence through $f(\theta)$ and $g(\theta)$, but also predicts the actual magnitude of observed changes in B^*. If, for instance, κ then Λ happened to be larger by a factor of 2, a 40% change in all data of Fig. 4 would result. In this sense our measurements appear as an indirect determination of the quantum of circulation κ.

The major part of this paper deals with vortex distribution effects. However, an important result concerning mutual friction is the clear experimental necessity of introducing a second dissipative coefficient B''. Further results on the axial attenuation, including temperature, pressure, and frequency dependence, will be published elsewhere. Measurements in variously shaped cavities confirm that at thermodynamic equilibrium the axial attenuation is proportional to the vortex density; the relevant coefficient, such as defined by Eq. (22), reproducibly takes the value $B''=0.021\pm0.001$ ($T=1.875$ K, $\omega/2\pi=200$ Hz). But we also observed metastable states for which the axial attenuation was strongly reduced. The metastable states cannot be attributed to the above-mentioned fluctuations in the vortex number which could affect the apparent value of B'' by only a few percent. We have not been able to explain this new kind of metastability in the framework of the HVBK model. We believe that the problem of the axial attenuation should require more refinements than merely introducing a third parameter B'' in the HVBK expression for the mutual-friction force.

[1] I. M. Khalatnikov, *Introduction to the Theory of Superfluidity* (Benjamin, New York, 1965), Chap. 16.
[2] P. Mathieu, J. C. Maréchal, and Y. Simon, Phys. Rev. B 22, 4293 (1980).
[3] P. Mathieu and Y. Simon, Phys. Rev. B 26, 1233 (1982).
[4] H. E. Hall and W. F. Vinen, Proc. R. Soc. London, Ser. A 238, 204 (1956); 238, 215 (1956).
[5] I. L. Bekarevich and I. M. Khalatnikov, Zh. Eksp. Teor. Fiz. 40, 920 (1961) [Sov. Phys.—JETP 13, 643 (1961)].
[6] H. A. Snyder and Z. Putney, Phys. Rev. 150, 110 (1966).
[7] J. Wilks, *The Properties of Liquid and Solid Helium* (Clarendon, Oxford, 1967), Chap. 13.2.
[8] F. London, *Macroscopic Theory of Superconductivity,* Vol. I of *Superfluids* (Dover, New York, 1961), p. 32.
[9] L. J. Campbell and R. M. Ziff, Phys. Rev. B 20, 1886 (1979).
[10] P. Mathieu and Y. Simon, Phys. Rev. Lett. 45, 1428 (1980).